Applied Rubber Belt Cover Loss Prediction from Indentation

Thomas J. Rudolphi*

INTRODUCTION

Efficient transport of bulk materials by belt conveyor systems is an important engineering design issue, especially as conveyors become longer and power requirements increase. It is well known within the industry that the parasitic energy loss of a belt conveyor, due to the indentation of the idlers into the belt backing material can be upwards of half the total energy required to drive it on a horizontal flight. Other loss sources includes the rolling resistance of the idlers, belt/roller misalignments, material trampling, frictional and acceleration losses on loading, etc., but energy absorbed by indentation of the belt backing as it passes over each successive idler is the dominant power consuming factor.

INDENTATION LOSS MODELS

Models to predict the rolling resistance of a cylinder (idler) on a viscoelastic foundation (backing material) have been available for some time. As a contact problem, it is nonlinear (contact length or indentation depth is a dependent on the load and vice versa) in load/deformation response. Rubber backing material is generally assumed to behave as a linear viscoelastic solid, even though it is known that most rubber compounds retain linearity only at very low strains. Because completely general solutions are impossible, practical solutions require simplifying assumptions. Those assumptions relate naturally to two separate parts of any analytical model:

1. The **deformation** model–aspects of the problem relating to the geometry, boundary conditions and kinematics of how the material deforms.
2. The **material** model–aspects of the problem relating to the material properties, or constitutive relationships, i.e., the stress/strain relationships.

For example, a simple deformation model is to assume that the belt backing deforms like a Winkler foundation, where the backing material behaves as a set of one-dimensional elements through the thickness, each behaving independently. By this assumption, there is no shear in the deformation model. For a simple material model it is often assumed that the backing behaves according to the simple 3-parameter Maxwell material, the so-called standard linear solid (SLS)–two springs and a dashpot in parallel.

To be specific, the early work of Jonkers [1] and Spaans [2] are both based on modeling the belt backing by a Winkler foundation. Four parameters–h, the backing thickness; D, the idler diameter; and W, the carry weigh or load per unit width of belt and the indentation depth–characterize this deformation. The material is characterized by the SLS model with storage and loss moduli E' and E'', and hence loss tangent $\tan(\delta) = E''/E'$, that are assumed to be independent of the loading frequency. The effective rolling resistance is determined by calculation of the energy absorbed by the backing material in the loading/unloading process during one pass over the idler. The lost energy would presumably go into heating of the backing material. Slightly different assumptions about how the energy per cycle is determined leads to slightly different results, but Jonkers' is representative and gives an indentation resistance factor,

$$f = \left(\frac{Wh}{E'D^2}\right)^{\frac{1}{3}} \frac{\pi}{2} \tan(\delta) \left[\frac{(\pi + 2\delta)\cos(\delta)}{4\sqrt{1 + \sin(\delta)}}\right]^{\frac{4}{3}} \qquad \text{EQ. 1}$$

It is observed that this Winker foundation/energy absorbed per cycle approach produces an indentation resistance factor proportional to $\tan(\delta)$. Thus, as might be expected, the loss tangent $\tan(\delta)$ is the important parameter in the rolling resistance factor.

As a more exact deformation model, Hunter [3] and May, et al. [4], presume the belt backing to be a two-dimensional viscoelastic half-plane, which, unlike and more general than the Winkler model, allows for shear deformation. In distinction to the Jonkers' and Spaan's approach these models calculate the rolling resistance by direct determination of the backing/idler interface stress,

* Iowa State University, Ames, Iowa.

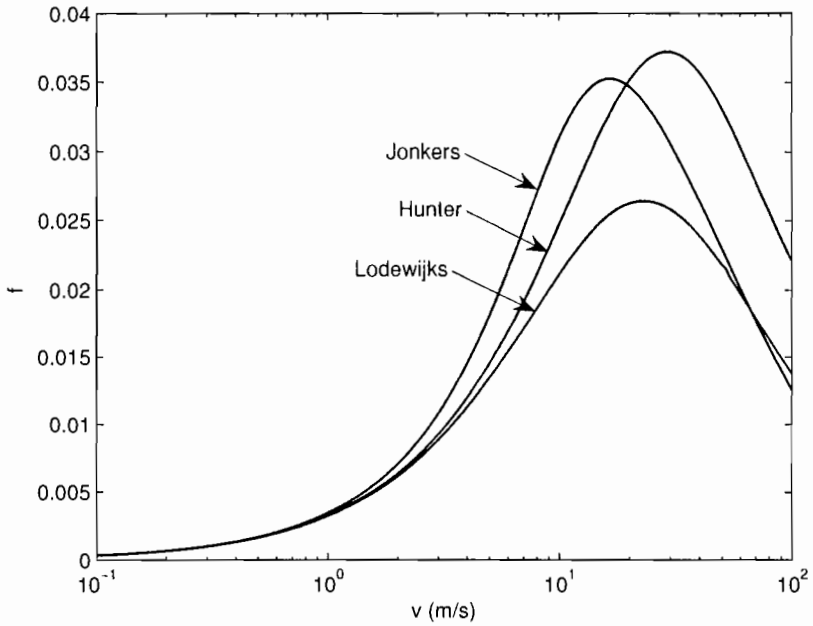

FIGURE 1 Indentation resistance by three methods with an SLS material model

assuming frictionless contact, and the moment of that normal stress about the idler axis. The rolling resistance is thus determined by the moment of the interface stress about the idler bearing. However, as based on a semi-infinite region, the backing thickness h is not inherently involved. The material model used by both Hunter and May is the simple three-parameter SLS.

This latter determination of the indentation resistance through the moment of the interface pressure is a more direct than the energy absorption approach of Jonkers and Spaans, since it circumvents the assumption of the lost energy per cycle absorbed by the backing by direct calculation of the moment of the interface stress. However, extension of this two-dimensional deformation model to more sophisticated materials beyond the relatively simple SLS, and finite backing thickness, is considerably more difficult. Full two-dimensional models with finite backing thickness require the solution of coupled integral equations as that of Margetson [6] or totally computational approaches such Wheeler [7] by finite elements or of Qiu [8] by boundary elements. The disadvantage of these numerical approaches is that solution dependence on critical parameters like roll radius, carry weight, backing thickness, etc., cannot be separated out explicitly as in equation (1).

Lodewijks [5] took an intermediate approach by using the Winkler foundation model for the backing, but determined the interface pressure between the roller and backing while using the SLS material model. This method is readily generalized to a more realistic material model and that has been done by Rudolphi and Reicks [9] for the generalized Maxwell, or Weichert model with $n + 1$ parameters. The form for that result may be written

$$f = \left(\frac{Wh}{E_0 R^2}\right)^{\frac{1}{3}} F(E_i, \tau_i) \qquad \text{EQ. 2}$$

where E_i and η_i are the elastic and dissipative elements of the Weichert model and $\tau_i = \eta_i/E_i$ are the characteristic periods of each element, E_0 is the long term stiffness value and $R = D/2$ is the idler radius. In equation (2), $F(E_i, \tau_i)$ denotes a function similar to that part of equation (1) involving δ, only somewhat more complex, but explicit form. While forms of equations (1) and (2) are similar, we observe that equation (2) is explicit in the Weichert parameters, while to use equation (1), the values of E' and $\tan(\delta)$ would have to be calculated from the material parameters. The relationships for that calculation is the Prony series forms of

$$E'(\omega) = E_0 + \sum_{i=1}^{n} E_i \frac{\omega^2 \tau_i^2}{1 + \omega^2 \tau_i^2}$$

$$E''(\omega) = \sum_{i=1}^{n} E_i \frac{\omega \tau_i}{1 + \omega^2 \tau_i^2} \qquad \text{EQ. 3}$$

The half space models of Hunter [3] and May [4] are difficult to extend from the SLS material to the Weichert model, but the Winkler foundation models that result in equations (1) and (2) are relatively simple to make this extension, hence allowing for more realistic rubber materials while requiring little more computational effort.

As an example, Figure 1 shows the indentation resistance results from three different deformation models with identical material models (SLS) for each. For the range of belt speeds considered, it is observed that the approach of Lodewijks provides lower values for the indentation resistance than the energy absorption approach of Jonkers, while the full two-dimensional solution of Hunter provides results which lay between the other two for lower values of belt speed. Lodewijks [5] provides a conversion factor to scale Winkler foundation results to the more exact half space models of

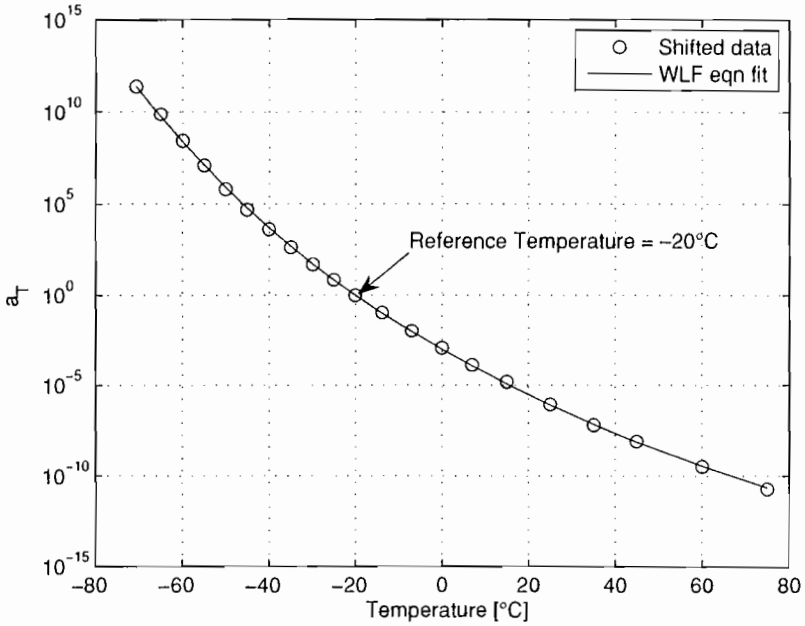

FIGURE 2 Frequency/temperature shift factor as a function of temperature

Hunter and May, which produces resistance values somewhere between the Lodewijks/Hunter curves of Figure 1.

Although the predictive models of indentation discussed above provide some variation in results, all are capable of providing relatively good estimates of the indentation resistance. The more analytically sophisticated models would logically provide better results, and to be sure, the computational solutions of Wheeler [7] and Qiu [8] would provide accurate predictions for finite backing thicknesses. Regardless of the approach, there are many aspects of the indentation phenomena that are not likely to be included, such as slippage and roughness at the interface, adhesion, etc. Similarly, the material model is likely to introduce its own assumptions and limitations. Thus, for this study, the method of Lodewijks [5], extended to the Weichert material model by Rudolphi and Reicks [9], will be used as the predictive model of indentation resistance.

BACKING MATERIAL CHARACTERIZATION

The mechanical properties of viscoelastic materials are typically measured by sinusoidal imposed deformations on specimens in simple tension, shear, bending or torsion at controlled temperatures and relatively low frequencies to avoid inertial effects. The time/temperature correspondence principle (cf. refs. [10] and [11]), which relates time or speed effects to temperature, allows one to extrapolate to frequencies and load rates considerably in excess of the test frequencies. In the frequency domain, the correspondence principle implies a shift factor a_T, which is determined from test data taken at a range of frequencies and a range of temperatures and then overlaying, through frequency shifts, the data at the different temperatures to form a "master" curve for a material. Examples of these graphs for typical backing rubber compound are shown in Figures 2 and 3.

A phenomenological basis for a_T in amorphous polymers is the Williams, Landel and Ferry [12], or WLF equation, $\log (a_T) = C_1(T - T_0)/[C_2 + (T - T_0)]$, where T is the temperature, T_0 is a reference temperature and C_1 and C_2 are constants determined by fitting the WLF equation to a_T as determined from the shifting to form the master curve. Figure 2 shows the shifted data and a least squares curve fit to the WLF equation.

The theory of linear viscoelasticity relates the stress and strain through relaxation or compliance functions and convolution integrals (adds up history effects). Standard characterization of the material by the Weichert model means determination of the constants (spectrum) E_i and $\tau_i = \eta_i/E_i$ of the Prony series of equations (3). Determination of that spectrum from experimental data, as embodied in a master curve like Figure 3, is a non-unique process, laden with several theoretical issues, but several methodologies (cf. Emery and Tschoegl [13]) have been developed to do this. Commercial software is also available for this purpose and rheological testing machines are often accompanied with data analysis software for that purpose. This issue is not the focus of this paper; it is presumed that the spectrum can be determined that faithfully reproduces the master curve data. The master curve data of Figure 3 shows the G' and G'' curves as reproduced by the spectrum developed by the author's own software—a least square, non-negative fit process at equally spaced period values τ_i through the frequency span of the data. The data represented in Figure 3 was taken by a standard rotational shear mode tests on thin tabs of the backing material.

A strong component of the indentation resistance, as evidenced in equation (1), is the material loss factor $\tan(\delta) = G''/G'$, as shown in Figure 4 for the above material. This curve is a typical shape for rubber compound properties used for belt backings in that it exhibits a fairly strong peak when plotted against the log of the frequency. Also, it is apparent that the master curve fit to the data may under or over-predict the data, due to

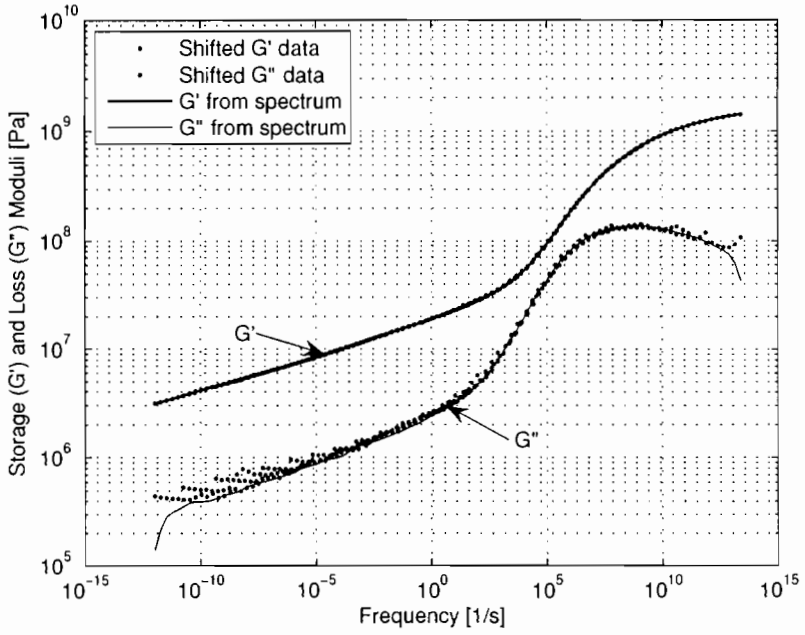

FIGURE 3 Typical master curves of shear storage and loss moduli

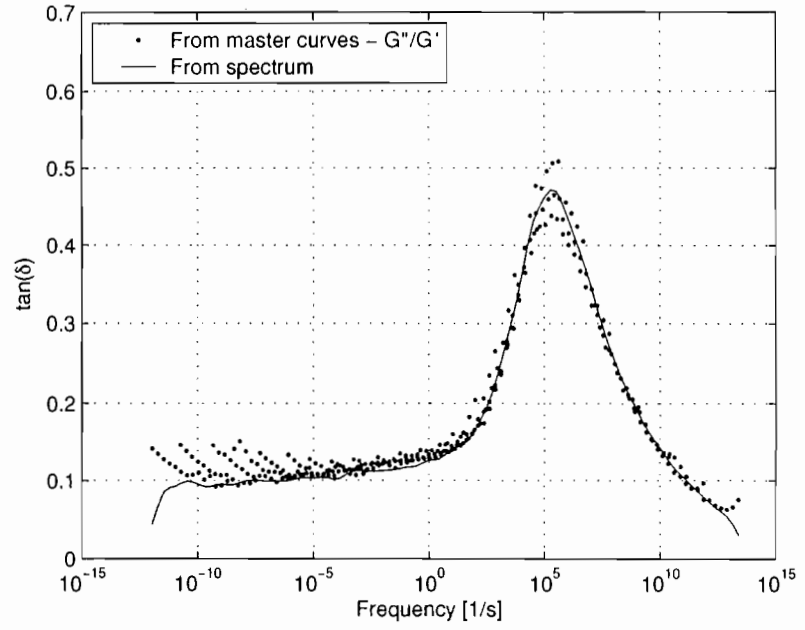

FIGURE 4 Loss tangent as a function of frequency

errors from several possible sources, but in this case is generally a good fit, which is important since the indentation resistance depends strongly on the loss tangent.

AN INDENTATION RESISTANCE EXAMPLE

The normalized indentation resistance factor $F = f/(WhE_0R^2)^{1/3}$ values for the above material as determined by both the equation of Jonkers, equation (1) and the extended method of Lodewijks, equation (2), with the Weichert material model is shown in Figure 5. The factor F is graphed vs. va_T, since on a logarithmic scale, the a_T-shifted values overlap for the full range of belt speeds and temperature due to the linear time/temperature superposition principle. Also, to reveal where a specific temperature determines values on the speed shifted scale through the shift factor a_T, shown on the right vertical axis is a plot of $\log(v)$ vs. va_T. On the logarithmic scale, these are the nearly vertical straight lines for a given temperature, or discrete values of a_T. Thus, to determine a value of F on this graph, at a given v and T, one starts with a specific V on the right

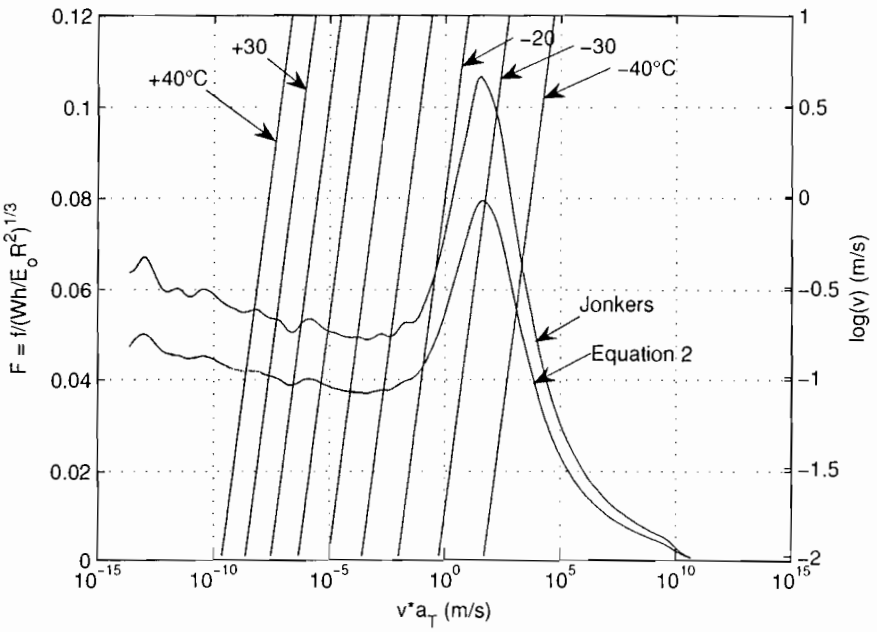

FIGURE 5 Indentation resistance as a function of belt speed and temperature

log(v) axis, follows it horizontally to the intersection of a specific temperature line of interest, then projects vertically, up or down, to the intersection with the curve to locate the F value corresponding to the given v and T. In this way, all indentation resistance values as a function of belt speed and temperatures are collapsed onto one curve.

As representative of a typical rubber backing material, it may be observed from Figure 5 that the predicted value of F, or f, at any given temperature, comes from a narrow range of the general curve, due to the nearly vertical log(v) lines. Alternately, for a given temperature, the variation in F comes from a small band on the curve as v varies, in this case, from nearly zero to 10 m/s. Thus F is relatively insensitive to v except at steep parts of the curve. We also observe the strong dependence on the loss tangent, due to the similarities of F in Figure 5 and the loss tangent tan(δ) of Figure 4. Presumably, the determination of F by a half-space model, by analogy to the results of Figure 1, would lie somewhere between the two curve, especially to the left of the peak.

From Figure 5, observe that the upper curve peaks at about v = 10 m/s and −25°C. At lower temperatures and higher belt speeds, one would drop down the resistance curve to the right. For most applications, one would not expect to exceed those conditions and at higher temperatures, one would be operating on the curves to the left of the peak. Within this lower range (higher temperatures and lower speeds) there is a possible variation in F from about 0.04 to 0.08, or a factor of two. For efficient design one may want to take advantage of that broad, relatively level region of these curves to the left of the peaks, while yet not ignoring the higher values in F at the lower temperatures and higher belt speeds.

SIMPLIFIED CURVES OF INDENTATION RESISTANCE FOR DESIGN

Based on the results and foregoing logic for the above representative material, a strategy for design for indentation resistance is suggested. One could create a design curve for F to be a simplification of Figure 5, within a practical range of interest, in the form of a "sigmoid,"

$$F = b_0 + b_1\{1 + \tanh[b_2 + b_3\log(va_T)]\} \qquad \text{EQ. 4}$$

where the four constants $b_0 \ldots b_3$ would be chosen to fit the normalized resistance curve in a "best" sense. Figure 6 shows such a sigmoid fit to the Jonkers' prediction of Figure 5 for use within a temperature range of about −20°C to +20°C. A similar curve could also be fit to the less conservative values of equation (2).

From such a simple parameterized curve of F as in Figure 6, the actual resistance factor f would be determined through the conversion $f = Wh/E_0R^2)^{1/3}F$ and the parameterized frequency/temperature shift factor a_T from Figure 2.

The F-curve parameterization process as described was performed for two other materials. Those results, fit to the equation (2) predictions, are shown in Figure 7 with the materials labeled (a), (b) and (c); material (a) being that of Figure 6. These could be considered low (a), intermediate (b) and higher (c) resistance compounds.

In this fashion, these types of generic material characteristic curves and associated parameters could then be used in a "design selection" or handbook fashion.

STRAIN AMPLITUDE EFFECTS

The effect of strain amplitude on the dissipative effects of rubber compounds is commonly known and strains larger than about 1% may often exceed the linear range (cf. Osanaiye [14]). For material (a) in the above study, along with measurements of the storage and loss moduli at low strain levels and a full range of temperatures and frequencies, the moduli were also measured at 3% strain, a frequency of 10 rad/sec and a range of temperatures. Figure 8 shows the effects on G' and G'' in a plot of each, normalized to their respective values at 0.01% strain, vs. % strain. The temperature dependent data is scattered, so there not a strict temperature

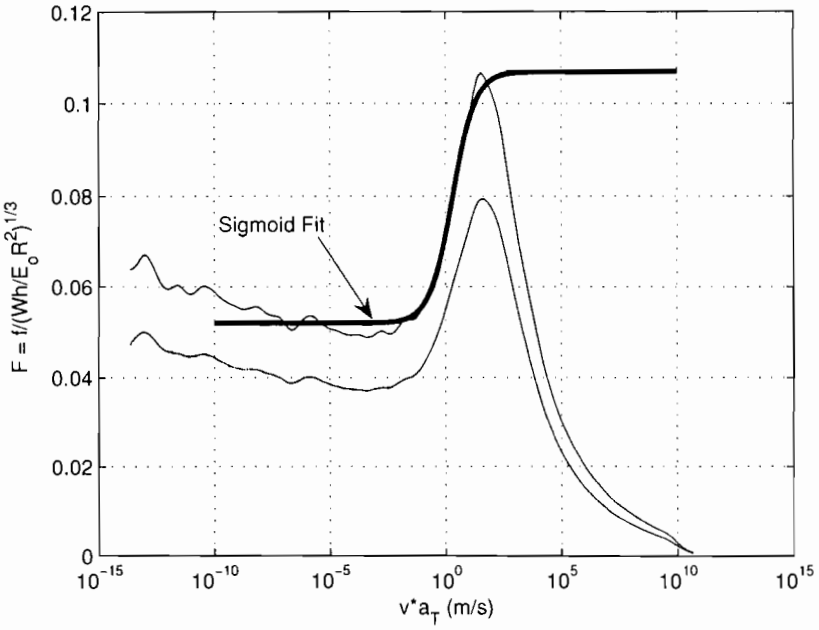

FIGURE 6 A sigmoid fit to the normalized indentation resistance factor

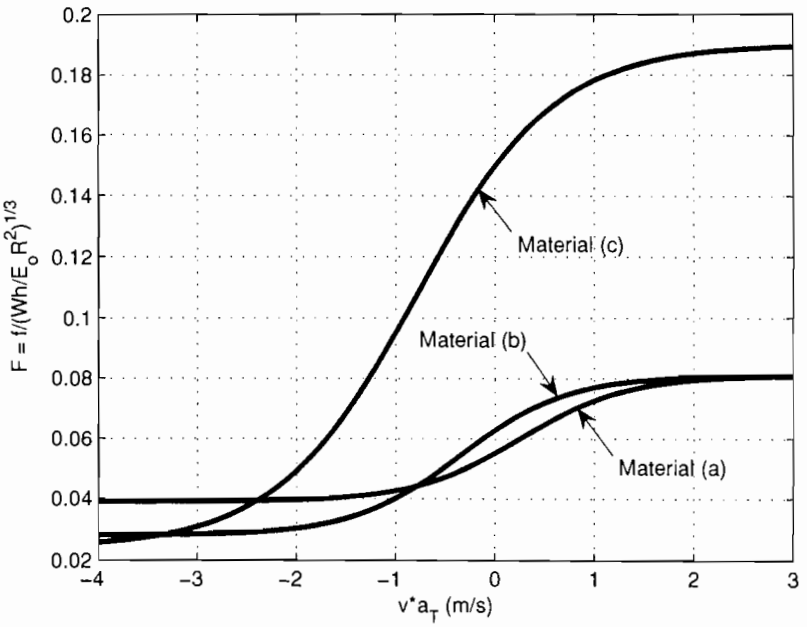

FIGURE 7 Sigmoid curves of normalized resistance factors for three materials

independence, but a polynomial is fit to both G' and G''. From the fitted curve it is clear that for strains greater than about 1%, G' decreases dramatically and G'' increases somewhat. Of course, with this trend, $\tan(\delta) = G''/G'$ varies proportionally with G'' and inversely with G'. It would be expected then, that at higher strain levels the loss tangent $\tan(\delta) = G''/G'$ would increase considerably. From Figure 8, there would be nearly a doubling of $\tan(\delta)$ at the higher strain values. Similar trends were observed in materials (b) and (c).

With an increased $\tan(\delta)$ at higher strain levels, the effect on the indentation resistance can roughly be gauged from equation (1), i.e., to first order effect, proportional to $\tan(\delta)$. The geometric parameters of the system, R and h, and the carry weight W also determined the strain in the backing material, but to a lower order than $\tan(\delta)$.

Using again the generalized method of Lodewijks with the material properties of material (a) as exemplified in Figures 2 through 8, strain amplitude corrections to the

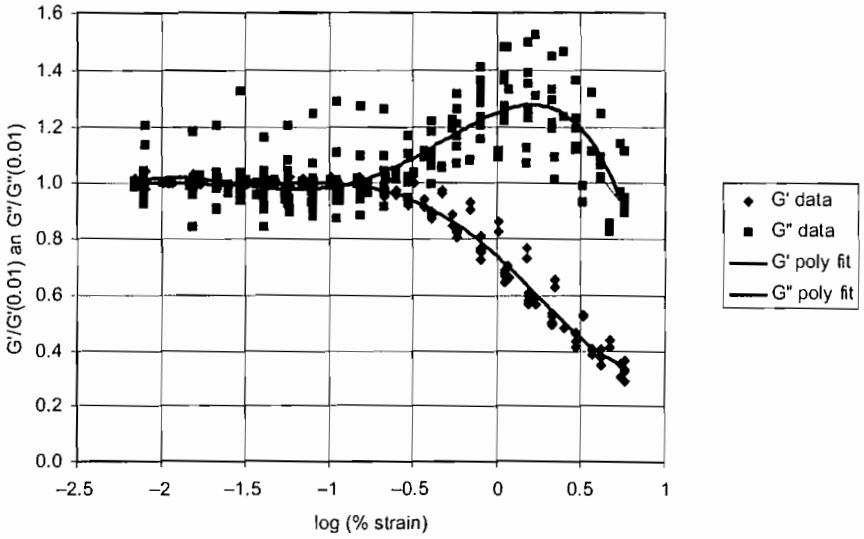

FIGURE 8 Strain amplitude effect on the shear storage and loss moduli

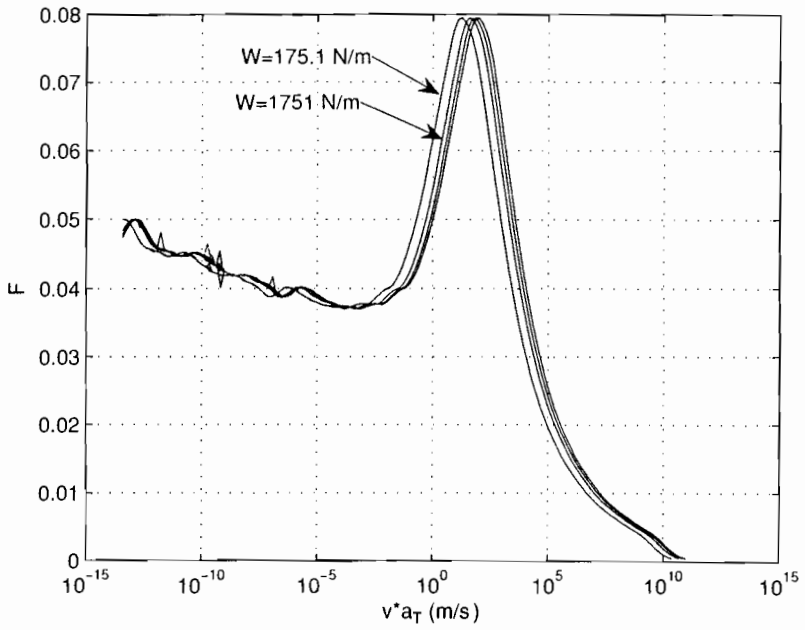

FIGURE 9 Normalized indentation resistance factor with strain amplitude correction

calculations required to evaluate the indentation resistance factor by equation (2) were performed. Now, however, as the strain is coupled to the parameters of the normalizing coefficient $(Wh/E_0R^2)^{1/3}$, i.e., W, h and R, the whole equation is evaluated. Since the maximum strain ε_0 of the Winkler backing increases with W, and decreases with h and R, to examine extreme values of f, the following calculations were made with small values of h = 0.006350 m = 0.25 in and R = 0.05080 m 2.0 in, while W takes on the four increasing values of W = [175.1; 1,751; 4,378; 8,756] N/m = [1, 10, 25, 50]lb/in. Figures 9 and 10 shows the normalized and non-normalized indentation factors resulting from the analysis.

The normalized factors are shown in Figure 9 where it is seen that four curves nearly overly one another, except for a small shift on the horizontal axis. The curve corresponding to the smallest W lies leftmost; the others proceed in order of increasing W to the right. The similarity of these curves is a consequence of using a continuously updated value of E_0 of equation (2) for each temperature and belt speed value, as required by the strain alteration of the material moduli, and tan(δ), as the calculation proceeds. This is to say that strain modulation of the material properties makes it essentially behave as different material, and the higher strains increase tan(δ) so that it responds more slowly, making the contact length shorter or increasing the load

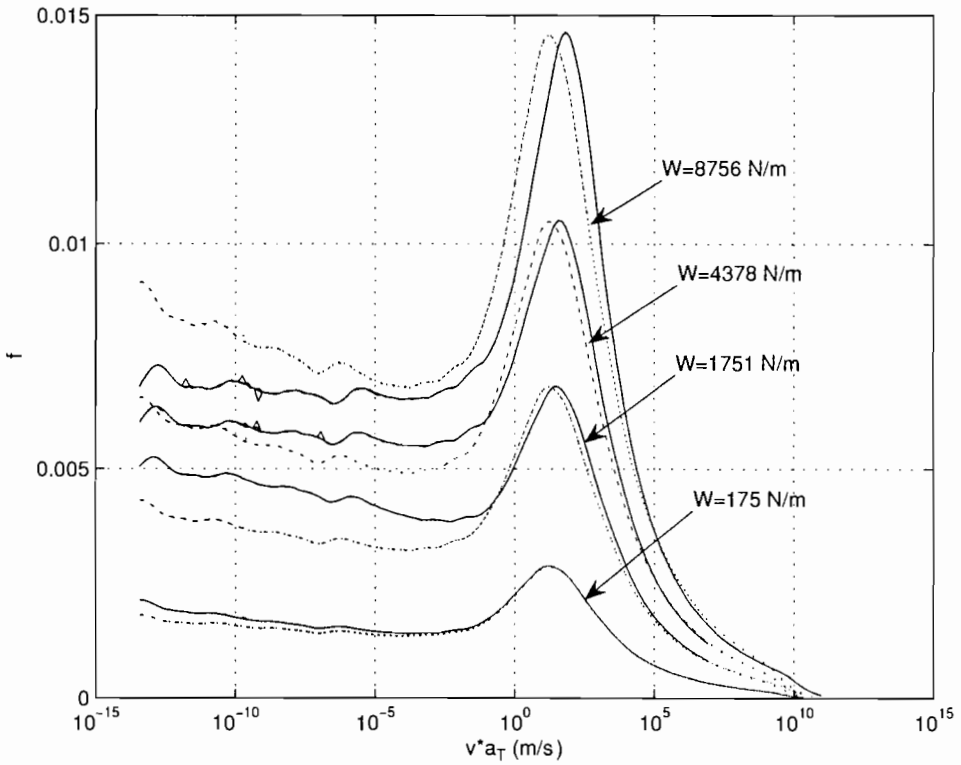

FIGURE 10 Indentation resistance factor with strain amplitude correction

frequency, shifting the curves to the right. Evidently the factor $F(E_i, \tau_i)$ of equation (2) is independent of strain amplification, other than the horizontal shift.

Figure 10 shows the un-normalized resistance factors by multiplication by $(Wh/E_0R^2)^{1/3}$ according to equation (2). The figure show two curves for each increment in the load W. The solid lines show the values as determined by equation (2) with the continuously updated E_0. The dashed lines show approximations to the same curves by using the low strain, normalized F curve of Figure 9 and a particular E_0 value chosen so as to produce equal values at the peak of the corresponding curves. Determination of that aligning E_0 value requires an iterative process, with strain correction, to determine the particular value of E_0 at the point where the F function peaks. Although this is nearly tantamount to direct determination of f, it has the important advantage of only requiring the one, low strain F curve of Figure 9. Further, the process is then amenable to the simplified sigmoid parameterization of Figure 7.

From the foregoing, we have then the ability to incorporate strain amplitude correction into the scheme of creating master and simplified curve for any material as in Figure 7. Values for the indentation factor f are then determined through a programmed process for any system parameters W, h and R, with the material parameters of a_T from the WLF equation for temperature location, remembering that for strain amplitude adjustment, the particular values of E_0 will also be required (an iteration, given W, h and R). Accordingly, an algorithm of small computational requirements can provide estimates of the indentation resistance for any material where the spectral properties are known.

The aforementioned iterative process could be based on the formula taken from Jonkers [1] methodology which relates maximum strain level ε_0 of the Winkler foundation (strain of that element directly under the idler), to W, h, R and E', i.e.,

$$\varepsilon_0 = \left[\frac{W(\pi/2 + \delta)\cos(\delta)}{2E'\sqrt{2Rh(1 + \sin(\delta))}}\right]^{\frac{2}{3}} \qquad \text{EQ. 5}$$

With this equation (5), for any given load and geometric parameters, and the strain amplification curves for the material like that of Figure 8, a small number of iterations on ε_0, given an initial estimate, determines a consistent values of E' and δ, and hence E_0 for that material and strain. By sweeping through the temperature and belt speeds of interest, while monitoring for the point where $\tan(\delta)$ is maximum, the appropriate value of E_0 is determined.

SUMMARY AND CONCLUSIONS

Fairly simple mechanical models of the indentation process are capable of providing good estimates of the indentation resistance. The basic methods based on the Winkler foundation assumption are easily extended to the general Weichert material model so realistic rubber compounds can also be included in the analysis. Under the assumptions of linear viscoelasticity, and the time/temperature correspondence principle, experimentally measured values of the dynamic storage and loss moduli at relatively low temperatures and modest frequency ranges can be used to

produce sufficiently high frequency data for simulating the indentation process. This paper shows how simplified characteristic indentation resistance factors can be developed for typical backing rubber and proposes that characteristic design curves be developed with an attendant algorithm for design calculations.

Under the Winkler foundation model for the backing material, strain amplitude effects on the material process can be included, although dependence of the material moduli on strain amplitude would be a violation of the linear viscoelastic assumption. We can incorporate this simple strain amplitude dependence into the material design curve methodology with little additional burden on computation.

Of course, the results of any analysis can be no more reliable than the material properties upon which it is based and for rubber belt backing materials, there are other, perhaps more influential issues to be considered, such as accuracy and reproducibility of measured material properties, evolutionary changes of the material properties due aging, the breaking-in transient, environmental influences, etc. The issue of strain amplitude correction is also based on assumptions that stretch the validity of linear viscoelasticity. Nevertheless, as more reliable material properties become available and testing methodologies become more standardized and reproducible, then the method outlined here by development of characteristic forms for various rubber compounds would serve to provide designers the ability to take advantage of lower power loss predictions.

REFERENCES

1. C.O. Jonkers, The indentation rolling resistance of belt conveyors: A theoretical approach, *Fördern und Heben*, 30, 4 (1980) 312-317.
2. C. Spaans, The calculation of the main resistance of belt conveyors, *Bulk Solids Handling*, 11, 4 (1991) 1-16.
3. S.C. Hunter, The rolling contact of a rigid cylinder with a viscoelastic half space, *Journal of Applied Mechanics*, 28 (1961) 611-617.
4. W.D. May, E.L. Morris and D. Atack, Rolling friction of a hard cylinder over a viscoelastic material, *Journal of Applied Physics*, 30, 11 (1959) 1713-1724.
5. G. Lodewijks, The rolling resistance of conveyor belts, *Bulk Solids Handling*, 15, 1 (1995) 15-22.
6. J. Margetson, Rolling contact of a rigid cylinder over a smooth elastic or viscoelastic Layer, *Acta Mechanica*, 13, 1-9, (1972), 1-9.
7. C.A. Wheeler, Analysis of the indentation rolling resistance of belt conveyors, *Proc. 7th Int. Conf. on Bulk Materials Storage, Handling and Transportation*, The Univ. of Newcastle, Australia, 559-567, Oct., 2001.
8. X. Qiu, A full two-dimensional model for rolling resistance: Hard cylinder on viscoelastic foundation of finite thickness, *Journal Engineering Mechanics, ASCE*, 132, 11 (2006).
9. T.J. Rudolphi and A.V. Reicks, Viscoelastic Indentation and Resistance to Motion of Conveyor Belts Using a Generalized Maxwell Model of the Backing Material, *Journal Rubber Chemistry and Technology*, June 2006.
10. A.S. Weinman and K.R. Rajagopal, *Mechanical Response of Polymers: An Introduction*, Cambridge University Press, Cambridge, UK, 2000.
11. J.D. Ferry, *Viscoelastic Properties of Polymers*, 3rd Edition, Wiley, New York, 1980.
12. M. Williams, R. Landel and J. Ferry, The temperature dependence of relaxation mechanisms in amorphous polymers and other glass-forming liquids, *Journal of the American Chemical Society*, 77 (1955), 3701.
13. I. Emri and N.W. Tschoegl, Generating line spectra from experimental responses. Part I: Relaxation modulus and creep compliance, *Rheologica Acta*, 32 (1993), 311-321.
14. G.J. Osanaiye, Effect of temperature and strain amplitude on dynamic properties of EPDM gum and its carbon black compounds, *Journal Applied Polymer Science*, 59, (1996), 567-575.